

# Kaon interferometry at KLOE/KLOE-2<sup>1</sup>

**Eryk Czerwiński**

Institute of Physics, Jagiellonian University, ul. Reymonta 4, 30-059 Cracow, Poland

E-mail: eryk.czerwinski@uj.edu.pl

**Abstract.** Neutral kaons from  $\phi$  meson decays are produced in pairs, which offers the possibility to select pure kaon beams: the detection of a  $K_S$  ( $K_L$ ) tags the presence of a  $K_L$  ( $K_S$ ), the same holds for charged kaons. This allows to perform precise measurement of kaon properties. Additionally, these neutral kaon pairs are produced in a pure quantum state ( $J^{PC} = 1^{--}$ ), which allows to investigate  $CP$  and  $CPT$  symmetries via quantum interference effects, as well as the basic principles of quantum mechanics.

Introduction to kaon interferometry and the results on the decoherence parameter and  $CPT$  test obtained by the KLOE experiment at the DAΦNE  $e^+e^-$  collider will be presented together with prospects for KLOE-2 project.

## 1. Introduction

The initial state of the two neutral kaons originated from  $\phi$  meson ( $J^{PC} = 1^{--}$ ) has to be antisymmetric and can be expressed as [1]:

$$|i\rangle = \frac{1}{\sqrt{2}} [ |K^0(+\vec{p})\rangle | \bar{K}^0(-\vec{p})\rangle - | \bar{K}^0(+\vec{p})\rangle | K^0(-\vec{p})\rangle ] \quad (1)$$

with the requirement:  $C|i\rangle = -|i\rangle$  and  $P|i\rangle = -|i\rangle$ . For the description of kaons production the strangeness basis can be used  $\{|K^0\rangle, |\bar{K}^0\rangle\}$ , while for the decay studies it can be changed to the  $\{|K_S\rangle, |K_L\rangle\}$  one:

$$|i\rangle = \frac{N}{\sqrt{2}} [ |K_S(+\vec{p})\rangle | K_L(-\vec{p})\rangle - | K_L(+\vec{p})\rangle | K_S(-\vec{p})\rangle ], \quad (2)$$

where  $N$  is a normalization factor equal to:

$$N = \frac{\sqrt{(1 + |\epsilon_S|^2)(1 + |\epsilon_L|^2)}}{1 - \epsilon_S \epsilon_L} \approx 1. \quad (3)$$

<sup>1</sup> On behalf of KLOE/KLOE-2 collaborations: D. Babusci, D. Badoni, I. Balwierz-Pytko, G. Bencivenni, C. Bini, C. Bloise, F. Bossi, P. Branchini, A. Budano, L. Caldeira Balkestahl, G. Capon, F. Ceradini, P. Ciambone, F. Curciarello, E. Czerwiński, E. Danè, V. De Leo, E. De Lucia, G. De Robertis, A. De Santis, A. Di Domenico, C. Di Donato, R. Di Salvo, D. Domenici, O. Erriquez, G. Fanizzi, A. Fantini, G. Felici, S. Fiore, P. Franzini, P. Gauzzi, G. Giardina, S. Giovannella, F. Gonnella, E. Graziani, F. Happacher, L. Heijkskjöld, B. Höistad, L. Iafolla, M. Jacewicz, T. Johansson, A. Kupsc, J. Lee-Franzini, B. Leverington, F. Loddo, S. Loffredo, G. Mandaglio, M. Martemianov, M. Martini, M. Mascolo, R. Messi, S. Miscetti, G. Morello, D. Moricciani, P. Moskal, F. Nguyen, A. Passeri, V. Patera, I. Prado Longhi, A. Ranieri, C. F. Redmer, P. Santangelo, I. Sarra, M. Schioppa, B. Sciascia, M. Silarski, C. Taccini, L. Tortora, G. Venanzoni, W. Wiślicki, M. Wolke, J. Zdebik

Since short- and long-lived states evolve in time as pure exponentials, the decay amplitude of such system can be presented as:

$$\begin{aligned} A(f_1, t_1; f_2, t_2) &= \frac{N}{\sqrt{2}} [\langle f_1|T|K_S(t_1)\rangle \langle f_2|T|K_L(t_2)\rangle - \langle f_1|T|K_L(t_1)\rangle \langle f_2|T|K_S(t_2)\rangle] = \\ &= \frac{N}{\sqrt{2}} \left[ \langle f_1|T|K_S\rangle \langle f_2|T|K_L\rangle e^{-i\lambda_S t_1} e^{-i\lambda_L t_2} - \langle f_1|T|K_L\rangle \langle f_2|T|K_S\rangle e^{-i\lambda_L t_1} e^{-i\lambda_S t_2} \right], \end{aligned} \quad (4)$$

where  $f_1$  and  $f_2$  denote decay final states at kaon proper times  $t_1$  and  $t_2$ ,  $T$  is the transition matrix and the eigenvalues:

$$\lambda_S = m_S - i\frac{\Gamma_S}{2} \quad \text{and} \quad \lambda_L = m_L - i\frac{\Gamma_L}{2}. \quad (5)$$

The double decay rate for  $\phi \rightarrow K^0 \bar{K}^0 \rightarrow f_1 f_2$  can be computed from equation (4):

$$\begin{aligned} I(f_1, t_1; f_2, t_2) &= |A(f_1, t_1; f_2, t_2)|^2 = C_{12} \left[ |\eta_1|^2 e^{-\Gamma_L t_1 - \Gamma_S t_2} + |\eta_2|^2 e^{-\Gamma_S t_1 - \Gamma_L t_2} + \right. \\ &\quad \left. - 2|\eta_1||\eta_2| e^{-\frac{(\Gamma_S + \Gamma_L)}{2}(t_1 + t_2)} \cos(\Delta m(t_1 - t_2) + \varphi_2 - \varphi_1) \right], \end{aligned} \quad (6)$$

where  $\varphi_1$  and  $\varphi_2$  are phases and:

$$\begin{aligned} C_{12} &= \frac{|N|^2}{2} |\langle f_1|T|K_S\rangle \langle f_2|T|K_S\rangle|^2, \\ \eta_i &= |\eta_i| e^{i\varphi_i} \equiv \frac{\langle f_i|T|K_L\rangle}{\langle f_i|T|K_S\rangle} \end{aligned} \quad (7)$$

and

$$\Delta m = m_L - m_S > 0 \quad \text{and} \quad \Delta\Gamma = \Gamma_S - \Gamma_L > 0. \quad (8)$$

For comparison of experimental data and above-mentioned theoretical evaluations the integration of the formula (6) over  $t = t_1 + t_2$  at a fixed difference of time  $\Delta t = t_1 - t_2$  can be done [1]:

$$\begin{aligned} I(f_1, f_2; \Delta t \geq 0) &= \frac{C_{12}}{\Gamma_S + \Gamma_L} \left[ |\eta_1|^2 e^{-\Gamma_L \Delta t} + |\eta_2|^2 e^{-\Gamma_S \Delta t} + \right. \\ &\quad \left. - 2|\eta_1||\eta_2| e^{-\frac{(\Gamma_S + \Gamma_L)}{2} \Delta t} \cos(\Delta m \Delta t + \varphi_2 - \varphi_1) \right], \end{aligned} \quad (9)$$

valid for  $\Delta t \geq 0$ , while for  $\Delta t < 0$  the substitutions  $\Delta t \rightarrow |\Delta t|$  and  $1 \leftrightarrow 2$  have to be applied.

Equation (9) implies that both kaons cannot decay at the same time in the same final state  $f_1 = f_2$ , and it is an example of correlation of the type pointed out for the first time by Einstein, Podolsky and Rosen [2] and the last line of this equation shows a time interference term which is a characteristic correlation between both kaon decays [1].

## 2. DAΦNE collider and KLOE experiment

The  $e^+e^-$  collider and  $\phi$ -factory DAΦNE is located in National Laboratory in Frascati (LNF-INFN, Italy). Electrons and positrons are accelerated in linac, then stored and cooled in an accumulator and finally transferred in bunches into separated storage rings with two interaction points [3]. A schematic view of DAΦNE complex is presented in Fig. 1. The collider was designed to operate at the peak of  $\phi$  resonance ( $\sqrt{s} = m_\phi \approx 1019 \text{ MeV}$ ). Since electrons and positrons

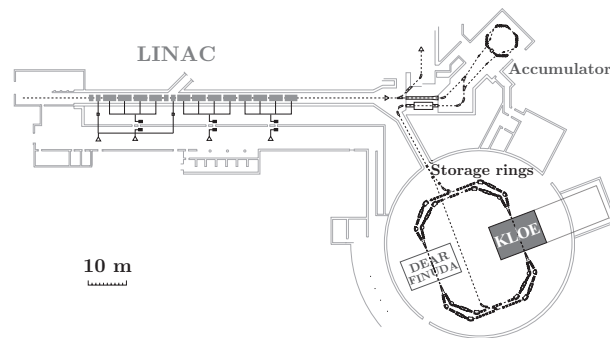


**Figure 1.** Scheme of the DAΦNE complex. A position of the KLOE detector at one of two interaction points is also presented. Figure taken from [4].

collide with small transverse momenta, the produced  $\phi$  mesons are almost at rest ( $\beta_\phi \approx 0.015$ ). A  $\phi$  meson decays mostly into kaon pairs (49% into  $K^+K^-$  and 34% into  $K_S K_L$ ), which makes a  $\phi$ -factory the natural place for kaon physics studies.

In years 2001-2006 KLOE has collected  $2.5 \text{ fb}^{-1}$  of integrated luminosity, which corresponds to about  $6.6 \times 10^9$  kaon pairs [5]. The detector itself consists of two main components: a  $\sim 3.3 \text{ m}$  long cylindrical drift chamber [6] with radius  $\sim 4 \text{ m}$  surrounded by an electromagnetic calorimeter [7]. Both sub-detectors are inserted in a superconducting coil which produces an axial magnetic field of  $0.52 \text{ T}$  parallel to the beam axis. Fig. 2 shows a schematic view of KLOE detector. The KLOE drift chamber was designed to detect a sizable fraction of  $K_L$  decays (mean

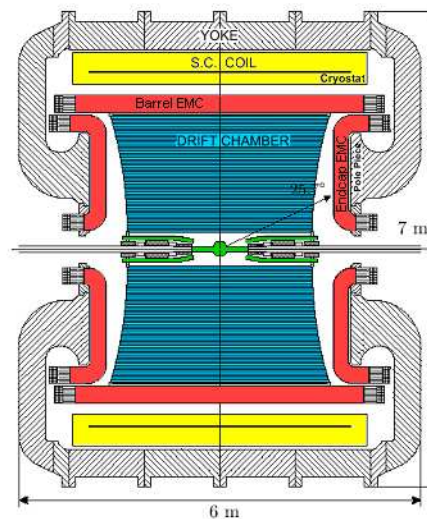


**Figure 2.** The KLOE detector surrounded by superconducting coil. Collision point of electrons and positrons is in the spherical beam-pipe in the center of the detector. Figure adapted from [4].

decay path of  $K_L$  meson is  $\sim 3.4 \text{ m}$ ). The chamber is filled with a mixture of helium and isobutane (90% and 10%, respectively) and has about 52000 wires arranged in cylindrical layers with alternate stereo angles. Based on the reconstruction of charged track curvature it allows for a fractional momentum accuracy of  $\sigma_p/p \approx 0.5\%$ . The resolution of vertex reconstruction is about  $1 \text{ mm}$ , while overall spatial accuracy is below  $2 \text{ mm}$ . An electromagnetic calorimeter consists of a barrel and side detectors (*endcaps*) providing almost  $4\pi$  coverage of solid angle. Each module

of calorimeter is read out on both sides by set of photomultipliers. It is build of stack of 1 mm scintillating fiber layers glued between grooved lead foils. The obtained accuracy of energy and time measurement are  $\sigma_E = 5.7\%/\sqrt{E[GeV]}$  and  $\sigma(t) = 54ps/\sqrt{E[GeV]} \oplus 100ps$ , respectively. Determination of the hit position in the plane transverse to the fiber direction is based on the analysis of signal amplitude distribution and the resolution is about 1 cm, while accuracy of longitudinal coordinate due to excellent time resolution amounts to  $\sigma_z = 1.2cm/\sqrt{E[GeV]}$ .

Since at KLOE kaons are produced in pairs from  $\phi$  decay, reconstruction of  $K_S$  decay close to interaction region (clean selection of  $K_S \rightarrow \pi^+\pi^-$ , BR=69%) allows for tagging of  $K_L$  presence. Having that and taking into account size of the detector itself makes KLOE an excellent place for  $K_L$  decay measurements. However, what is even more important, detection of  $K_L$  hit in calorimeter module tags the presence of  $K_S$ . This method makes KLOE an unique place to study pure  $K_S$  beams. This method was recently used for the most precise determination of the upper limit of  $BR(K_S \rightarrow \pi^0\pi^0\pi^0)$  [8].

### 3. Decoherence parameter

The transition of a pure state into an incoherent mixture of states is generally denoted as decoherence [1], meaning that entanglement of particles is lost. The decoherence parameter  $\zeta$  can be introduced by multiplying the interference term in equation (6) by a factor  $(1 - \zeta)$ :

$$I(f_1, t_1; f_2, t_2) = C_{12} \left[ |\eta_1|^2 e^{-\Gamma_L t_1 - \Gamma_S t_2} + |\eta_2|^2 e^{-\Gamma_S t_1 - \Gamma_L t_2} + 2(1 - \zeta) |\eta_1| |\eta_2| e^{-\frac{(\Gamma_S + \Gamma_L)}{2}(t_1 + t_2)} \cos(\Delta m(t_1 - t_2) + \varphi_2 - \varphi_1) \right]. \quad (10)$$

Figure 3 shows sensitivity of the double decay rate distribution to the value of  $\zeta$  in the case  $f_1 = f_2 = \pi^+\pi^-$ . The biggest discrepancy can be observed for  $\Delta t$  close to 0. The quantum mechanics case is described without decoherence ( $\zeta = 0$ ), while the total decoherence corresponds to  $\zeta = 1$ , so kaons are no longer entangled. Intermediate situations between these two correspond to values of  $\zeta$  within the range (0,1).

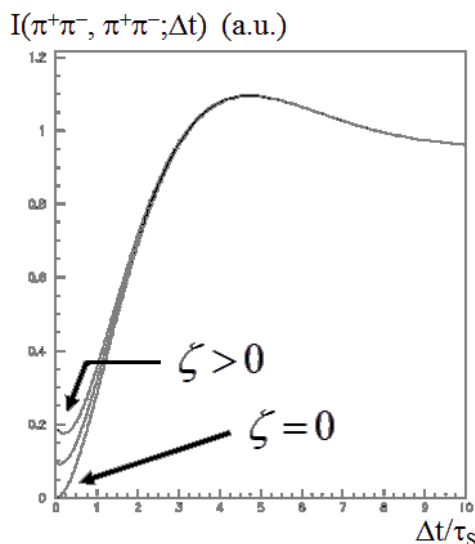


**Figure 3.** The  $I(\pi^+\pi^-, \pi^+\pi^-, \Delta t)$  distribution for quantum mechanic case ( $\zeta = 0$ ), and for two greater than zero values of the decoherence parameter. The biggest discrepancy is for  $\Delta t$  close to 0. The figure is taken from [1]

Based on the integrated luminosity of  $\approx 1.5 \text{ fb}^{-1}$  study of the decoherence parameter was performed at KLOE [9]. The signal events  $\phi \rightarrow K_S K_L \rightarrow \pi^+ \pi^- \pi^+ \pi^-$  were selected by requirement of two vertexes, each with two opposite-curvature tracks inside the drift chamber, with an invariant mass and total momentum compatible with the two neutral kaon decays. The experimental points were fitted with Eq. 11 modified with parameters expressing decoherence in different models described in [1,9]. The fit was performed taking into account resolution and detection efficiency, the background from coherent and incoherent  $K_S$  regeneration on the beam pipe wall, and the small contamination from the non-resonant  $e^+ e^- \rightarrow \pi^+ \pi^- \pi^+ \pi^-$  channel. The determined experimental distribution of the  $\phi \rightarrow K_S K_L \rightarrow \pi^+ \pi^- \pi^+ \pi^-$  intensity as a function of the absolute value of  $\Delta t$  is shown in Fig. 4. The results:

$$\begin{aligned} \zeta_{SL} &= (0.3 \pm 1.8_{stat} \pm 0.6_{syst}) \cdot 10^{-2} , \\ \zeta_{0\bar{0}} &= (1.4 \pm 9.5_{stat} \pm 3.8_{syst}) \cdot 10^{-7} , \end{aligned} \quad (11)$$

where  $\zeta_{SL}$  and  $\zeta_{0\bar{0}}$  depend on the basis in which the initial state is expressed:  $\{|K^0\rangle, |\bar{K}^0\rangle\}$  or  $\{|K_S\rangle, |K_L\rangle\}$ , show no deviation from quantum mechanics [9].

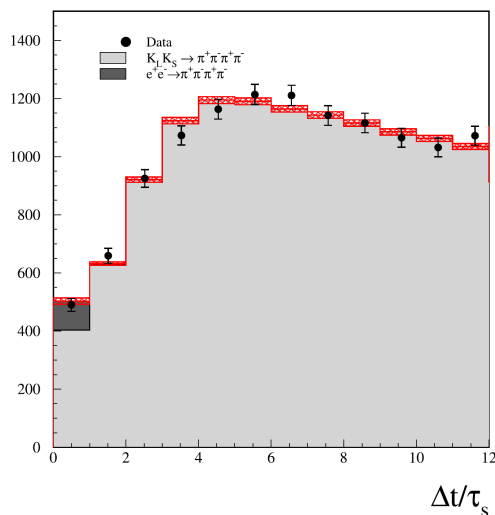


**Figure 4.** Points denote experimental results, while fitted histogram shows results of the Monte Carlo simulation. The bin size corresponds to the time resolution  $\sigma(\Delta t) \approx \tau_S$  [9].

#### 4. CPT, QM and Lorentz symmetry breaking

*CPT* invariance is a fundamental theorem in the framework of quantum field theory (QFT), as a consequence of Lorentz invariance, unitarity and locality. In several quantum gravity (QG) models, however, *CPT* can be violated via some mechanism which can also violate standard Quantum Mechanics (QM). In a review Bernabeu, Ellis, Mavromatos, Nanopoulos and Papavassiliou [10] discuss the theoretical motivations for possible *CPT* violations and the unique role played by the entangled neutral kaon pairs produced at DAΦNE in precision tests of the *CPT* symmetry.

As an example of this incredible precision reachable with neutral kaons, the model by Ellis, Hagelin, Nanopoulos and Srednicki (EHNS) which introduces three *CPT* and QM-violating real parameters  $\alpha$ ,  $\beta$  and  $\gamma$  [11] can be used. On phenomenological grounds, they are expected to be  $O(m_K^2/M_{Pl}) \sim 2 \times 10^{-20} \text{ GeV}$  at most, since  $M_{Pl} \sim 10^{19} \text{ GeV}$ , the Plank mass. Interestingly

enough, this model give rise to observable effects in the behavior of entangled neutral meson systems, as shown also in [12], that can be experimentally tested.

KLOE has already published competitive results on these issues [13], based on a statistics of  $\sim 400 \text{ pb}^{-1}$ , and is now on the way of updating them using the full data sample.

The *CPT* symmetry breaking at KLOE could be also observed using kaon interferometry with both kaons decaying in  $\pi^+\pi^-$  pairs. The refined analysis with additional data have brought the results on decoherence and *CPT*-violating parameters presented in Ref. [9]. A general theoretical possibility for *CPT* violation is based on spontaneous breaking of Lorentz symmetry, as developed by Kostelecky [14–16] in the *Standard-Model Extension* (SME). KLOE has already performed a preliminary analysis [9] using only half of the total available statistics ( $1 \text{ fb}^{-1}$ ). In this analysis the forward-backward asymmetry along *Z* direction as a function of sidereal time only was used. With this approach only the vector part of the  $\Delta a_\mu$  four-vector can be observed. The preliminary results on  $\Delta a_{X,Y,Z}$  are:

$$\begin{aligned}\Delta a_X &= (-6.3 \pm 6.0) \times 10^{-18} \text{ GeV}, \\ \Delta a_Y &= (2.8 \pm 5.9) \times 10^{-18} \text{ GeV}, \\ \Delta a_Z &= (2.4 \pm 9.7) \times 10^{-18} \text{ GeV}.\end{aligned}$$

A new analysis of the  $K_L K_S \rightarrow \pi^+\pi^-\pi^+\pi^-$  final state is in progress to improve the SME parameters, through the measurement of the decay amplitude as a function of the delay between kaon decays, ordered according to the quadrant in the celestial coordinate frame [17]. The reconstruction of events in the region  $\Delta t \approx 0$  is crucial for the precision measurement of the interference term.

## 5. KLOE–2 project

In 2011 the KLOE–2 detector, a successor of KLOE, has started data taking campaign in order to extend KLOE physics program [18].

The test of fundamental symmetries and Quantum Mechanics coherence of the neutral kaon system, and the search for phenomena beyond the Standard Model are the main motivations for KLOE–2. Thanks to the luminosity upgrade of DAΦNE, as well as ongoing installation of new detectors, KLOE–2 will be able to improve the accuracy of the measurement of the  $K_S$  meson properties and to study the time evolution of the entangled pairs of neutral kaons with an unprecedented precision. The significant improvement of the sensitivity of the tests of the discrete symmetries in the decays of  $K$ ,  $\eta$  and  $\eta'$  mesons beyond the presently achieved limits is expected. Good accuracy of reconstruction of  $K_L$  decays in large fiducial volume was a base for the physics program of KLOE. At KLOE–2 an increased interest will be focused on the physics close to the interaction point (IP) as rare  $K_S$  decays,  $K_S - K_L$  interference, multi-lepton events, as well as  $\eta$ ,  $\eta'$  and  $K^\pm$  decays. Detailed KLOE–2 physics program can be found in Ref. [18].

In 2011 the new interaction region of electron and positron beams consists on the Crabbed Waist compensation of the beam-beam interaction with large Piwinski angle and small beam sizes was successfully commissioned [19]. Upgraded DAΦNE allows to increase delivered luminosity (with unchanged beam current) by a factor of three with respect to the performance reached before the upgrade.

Apart of the collider the detector itself was also upgraded. Two pairs of small angle tagging devices [20] to detect low (Low Energy Tagger - LET) [21] and high (High Energy Tagger - HET) energy  $e^+e^-$  originated from  $e^+e^- \rightarrow e^+e^-X$  reactions was installed. This tagger system allows to perform the studies of  $\gamma\gamma$  physics. In the next step a light-material Inner Tracker detector based on the Cylindrical GEM technology will be installed in the region between the beam pipe and the drift chamber to improve charged vertex reconstruction and to increase the acceptance for low transverse momentum tracks [22, 23]. In addition, crystal calorimeters (CCALT) will cover the low polar  $\theta$  angle region to increase acceptance for very forward electrons and photons

down to  $8^\circ$  [24]. A new tile calorimeter (QCALT) will be used for the detection of photons coming from  $K_L$  decays in the drift chamber [25].

Figure 5 presents the comparison between results obtained with present spatial resolution and after installation of Inner Tracker for decoherence studies. An improved sensitivity on decoherence parameters of about one order of magnitude is expected with higher collected statistics and the use of Inner Tracker.

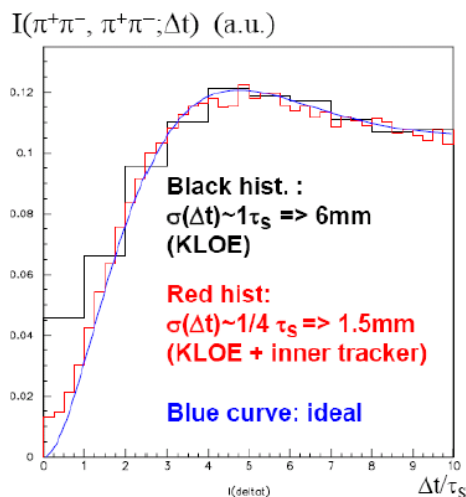


**Figure 5.** Comparison of the  $I(\pi^+\pi^-, \pi^+\pi^-, \Delta t)$  distribution obtained with KLOE resolution and after Inner Tracker insertion based on the Monte Carlo simulation.

## 6. Summary

The KLOE experiment obtained already several significant and precise results in kaon physics [5], due to the unique possibility of producing pure  $K_L$ ,  $K_S$  and  $K^\pm$  beams. The success of the DAΦNE upgrade was a motivation to start a new experiment, KLOE-2, which aims to complete and extend the KLOE physics program. LET and HET tagging systems have been already installed and the first phase of new data taking campaign has started. After installation of new set of detectors (namely Inner Tracker, QCALT and CCALT calorimeters) new phase of data taking will start in 2013 for precise measurements of rare decays of kaon,  $\eta$  and  $\eta'$ , as well as CP and CPT tests and kaon interferometry studies. The accuracy in the measurements is expected in most cases to be improved by about one order of magnitude [18].

## Acknowledgments

The author would like to express his appreciation to Giorgio Giardina and Giuseppe Mandaglio for invitation and hospitality. The author acknowledges the support of the Polish National Science Centre through the Grant No. 2011/01/D/ST2/00748 and the Foundation for Polish Science through the project HOMING PLUS BIS/2011-4/3.

## References

- [1] *Handbook on neutral kaon interferometry at a Phi-factory*, editor: A. Di Domenico, Frascati Physics Series **43** (2007).
- [2] A. Einstein, B. Podolsky, N. Rosen, *Physical Review* **47**, 777 (1935).
- [3] The  $\phi$ -factory Study Group *Proposal for a  $\phi$ -factory*, LNF-90/031 (R) (1991).
- [4] P. Franzini and M. Moulson, *Ann. Rev. Nucl. Part. Sci.* **56**, 207 (2006).

- [5] F. Bossi, E. De Lucia, J. Lee-Franzini, S. Miscetti, M. Palutan and KLOE Collaboration, *Rivista del Nuovo Cimento* Vol.31, N.10 (2008).
- [6] M. Adinolfi *et al.* (KLOE), *Nucl. Instr. & Meth.* **488**, 51 (2002).
- [7] M. Adinolfi *et al.*, *Nucl. Instr. & Meth. A* **482**, 364 (2002).
- [8] M. Silarski, PhD Thesis, Cracow (2012).
- [9] A. Di Domenico *et al.* [KLOE Collaboration], *J. Phys. Conf. Ser.* **171**, 012008 (2009).
- [10] J. Bernabeu, J. Ellis, N.E. Mavromatos, D.V. Nanopoulos and J. Papavassiliou, arXiv:hep-ph/0607322, in Ref. [1].
- [11] J. Ellis, J.S. Hagelin, D.V. Nanopoulos, M. Srednicki, *Nucl. Phys. B* **241**, 381 (1984).
- [12] P. Huet, M. Peskin, *Nucl. Phys. B* **434**, 3 (1995).
- [13] F. Ambrosino *et al.*, (KLOE Collaboration) *Phys. Lett. B* **642**, 315 (2006).
- [14] V.A. Kostelecký, *Phys. Rev. Lett.* **80**, 1818 (1998).
- [15] V.A. Kostelecký, *Phys. Rev.* **D61**, 016002 (1999).
- [16] V.A. Kostelecký, *Phys. Rev.* **D64**, 076001 (2001).
- [17] A. De Santis, PoS (HQL 2012) 018 (2012).
- [18] G. Amelino-Camelia *et al.*, *Eur. Phys. J. C* **68**, 619-681 (2010).
- [19] M. Zobov *et al.*, *Phys. Rev. Lett.* **104**, 174801-174806 (2010).
- [20] F. Archilli *et al.*, *Nucl. Instr. & Meth. A* **617**, 266 (2010).
- [21] D. Babusci *et al.*, *Nucl. Instr. & Meth. A* **617**, 81 (2010).
- [22] KLOE-2 Collaboration, F. Archilli *et al.*, LNF-10/3(P) INFN-LNF, arXiv:1002.2572
- [23] A. Balla *et al.*, *Nucl. Instr. & Meth. A* **604**, 23 (2009).
- [24] M. Cordelli *et al.*, *Nucl. Instr. & Meth. A* **617**, 109 (2010).
- [25] M. Cordelli *et al.*, *Nucl. Instr. & Meth. A* **617**, 105 (2010).